The EMBO Journal (2010) 29, 3408–3420 | © 2010 European Molecular Biology Organization | All Rights Reserved 0261-4189/10
www.embojournal.org

THE EMBO JOURNAL

Neurotoxicity of Alzheimer's disease Aβ peptides is induced by small changes in the $Aβ_{42}$ to $Aβ_{40}$ ratio

Inna Kuperstein[1,2,10,12], Kerensa Broersen[3,4,10], Iryna Benilova[1,2,5,10], Jef Rozenski[6], Wim Jonckheere[3,4], Maja Debulpaep[3,4], Annelies Vandersteen[3,4], Ine Segers-Nolten[7], Kees Van Der Werf[7], Vinod Subramaniam[7], Dries Braeken[5], Geert Callewaert[5], Carmen Bartic[5,8], Rudi D'Hooge[9], Ivo Cristiano Martins[3,4,11], Frederic Rousseau[3,4,*], Joost Schymkowitz[3,4,*] and Bart De Strooper[1,2,*]

[1]Department for Molecular and Developmental Genetics, Flanders Institute for Biotechnology (VIB), Leuven, Belgium, [2]Center for Human Genetics, KULeuven, Leuven, Belgium, [3]Switch Laboratory, Flanders Institute for Biotechnology (VIB), Brussels, Belgium, [4]Vrije Universiteit Brussel (VUB), Brussels, Belgium, [5]IMEC, Bioelectronic Systems Group, Heverlee, Belgium, [6]Laboratory of Medicinal Chemistry, Rega Institute for Medical Research, Leuven, Belgium, [7]Faculty of Science and Technology, Nanobiophysics, MESA+ Institute for Nanotechnology, MIRA Institute for Biomedical Technology and Technical Medicine, University of Twente, Enschede, The Netherlands, [8] Department of Physics and Astronomy, Laboratory of Solid State Physics and Magnetism, KULeuven, Belgium and [9]Laboratory of Biological Psychology, KULeuven, Leuven, Belgium

The amyloid peptides $Aβ_{40}$ and $Aβ_{42}$ of Alzheimer's disease are thought to contribute differentially to the disease process. Although $Aβ_{42}$ seems more pathogenic than $Aβ_{40}$, the reason for this is not well understood. We show here that small alterations in the $Aβ_{42}$:$Aβ_{40}$ ratio dramatically affect the biophysical and biological properties of the Aβ mixtures reflected in their aggregation kinetics, the morphology of the resulting amyloid fibrils and synaptic function tested *in vitro* and *in vivo*. A minor increase in the $Aβ_{42}$:$Aβ_{40}$ ratio stabilizes toxic oligomeric species with intermediate conformations. The initial toxic impact of these Aβ species is synaptic in nature, but this can spread into the cells leading to neuronal cell death. The fact that the relative ratio of Aβ peptides is more crucial than the absolute amounts of peptides for the induction of neurotoxic conformations has important implications for anti-amyloid therapy. Our work also suggests the dynamic nature of the equilibrium between toxic and non-toxic intermediates.

The EMBO Journal (2010) **29,** 3408–3420. doi:10.1038/emboj.2010.211; Published online 3 September 2010
Subject Categories: neuroscience; molecular biology of disease
Keywords: Alzheimer's disease; β-amyloid peptides; microelectrode array; neurotoxicity; oligomer

Introduction

Amyloid β (Aβ) peptides generated from the amyloid precursor protein (APP) by β- and γ-secretase-mediated cleavage (Annaert and De Strooper, 2002) are thought to have an important function in the neurodegenerative process in Alzheimer's disease (AD) (Hardy and Selkoe, 2002). γ-Secretase cleavage of APP generates a heterogeneous mixture of Aβ peptides varying in length at their carboxytermini (Sato *et al*, 2003; Qi-Takahara *et al*, 2005; Kakuda *et al*, 2006). Additional heterogeneity is generated at the aminoterminus by aminopeptidases, glutaminylcyclases and other modifications (Pike *et al*, 1995; Saido *et al*, 1996) (reviewed in De Strooper, 2010). It has been proposed that some of these variations might contribute to the neurotoxic properties of Aβ peptides (Schilling *et al*, 2008).

The major Aβ species recovered from serum, cerebrospinal fluid and cell culture supernatants is 40 amino acids long ($Aβ_{40}$) (Haass and Selkoe, 1993; Scheuner *et al*, 1996). Interest in a second peptide, $Aβ_{42}$, which is detected at about 10-fold lower levels, was strongly stimulated by the observation that familial AD causing mutations in the APP gene and/or in the gene encoding the γ-secretase complex component presenilin increased the relative production of $Aβ_{42}$ relative to $Aβ_{40}$ (Suzuki *et al*, 1994; Duff *et al*, 1996; Scheuner *et al*, 1996). We reported earlier (Bentahir *et al*, 2006) that clinical mutations in presenilin do not necessarily increase the production of Aβ, but that they mainly affect the spectrum of the Aβ peptides generated by γ-secretase. As patients with presenilin mutations present an early and aggressive form of the disease, it seems then logical to propose that the absolute quantity of Aβ peptides produced in the brain might be less important than the quality of the Aβ peptides (reflected in a changed $Aβ_{42}$ to $Aβ_{40}$ ratio) for the generation of elusive toxic Aβ species (De Strooper, 2007). The implications of such hypothesis for current efforts in drug development is important because lowering the absolute amounts of Aβ in patients would then be less crucial than the restoration of the correct ratios of Aβ peptides. Earlier studies have already provided evidence that $Aβ_{40}$ and $Aβ_{42}$ affect each other's aggregation rates and toxic effects (Snyder *et al*, 1994; Frost *et al*, 2003; Yoshiike *et al*, 2003; Wang *et al*, 2006; Kim *et al*, 2007; Yan and Wang, 2007; Jan *et al*, 2008). Generally, it is found that $Aβ_{42}$ has fast aggregation kinetics,

*Corresponding authors. F Rousseau or J Schymkowitz, Switch Laboratory, Flanders Institute for Biotechnology (VIB) and Vrije Universiteit Brussel (VUB), Pleinlaan 2, Brussels 1050, Belgium. Tel.: +322 629 1025; Fax: +322 629 1942;
E-mails: frederic.rousseau@switch.vib-vub.be or joost.schymkowitz@switch.vib-vub.be or B De Strooper, Center for Human Genetics, Flanders Institute for Biotechnology (VIB) and KULeuven, Herestraat 49, Leuven 3000, Belgium. Tel.: +321 634 6227; Fax: +321 634 7181; E-mail: bart.destrooper@med.kuleuven.be
[10]The authors contributed equally to this work
[11]Present address: Biomembranes Unit, Institute de Medicina Molecular (IMM), Av. Prof. Egas Moniz, Lisboa, Portugal
[12]Present address: Institut Curie, Département de Transfert, and INSERM, U900, Paris F-75248 France

Received: 28 January 2010; accepted: 3 August 2010; published online: 3 September 2010

which can be inhibited by $A\beta_{40}$ in a concentration-dependent manner. Interesting *in vivo* studies have further shown that increased levels of $A\beta_{40}$ peptides in the brain actually might have a protective effect (Wang *et al*, 2006; Kim *et al*, 2007).

In the past, a lot of attention has gone to the accumulation of Aβ in plaques and the relationship between amyloid plaques and AD. However, little or no correlation was found between the total burden of Aβ peptide deposited into plaques in the brain and the degree of neurodegeneration in the patients (Terry *et al*, 1991; Price and Morris, 1999). More recently, this discrepancy has been confirmed with modern amyloid imaging techniques (Aizenstein *et al*, 2008; Reiman *et al*, 2009). Obviously, it is possible that these patients are in a preclinical phase of the disease, and follow-up studies are underway to investigate this. Nevertheless, these observations support the concept that the amyloid fibrils are biologically largely inert and that not all conformations of Aβ are equally toxic (Martins *et al*, 2008; Shankar *et al*, 2008). A series of intermediate soluble aggregates of Aβ peptides, such as 'Aβ-derived diffusible ligands' (ADDLs) (Lambert *et al*, 1998) or 'natural toxic oligomers' (Walsh *et al*, 2002), have been identified. The mechanism of their neurotoxic activity remains not only subject of intense investigation, but also the precise conformation(s) of the toxic species remains uncertain (Kayed *et al*, 2003; Hepler *et al*, 2006). Dimers were proposed to potently disrupt synaptic plasticity (Klyubin *et al*, 2008; Shankar *et al*, 2008), an Aβ species of 56 kDa has been found neurotoxic in Tg2576 mice (Lesne *et al*, 2006), lipid-induced oligomers from mature fibrils (Martins *et al*, 2008), ADDLs (Lambert *et al*, 1998; Gong *et al*, 2003; Lacor *et al*, 2007) and annular assemblies (Lashuel *et al*, 2002) were shown to exert neurotoxic effects, affect synapse function and even memory formation in mice. It should be noted that in many of the publications, the identified toxic species are presented as stable, defined structures, although it seems logical to assume that their assembly and disassembly is a dynamic and continuous process, at least in the initial stages, and the alternative possibility that toxicity is present over a series of conformers or sizes should not be disregarded (Hepler *et al*, 2006; Martins *et al*, 2008; Ono *et al*, 2009). Toxicity seems to be higher with tetramers than dimers for instance (Ono *et al*, 2009). The question is thus how biophysical parameters influence this process *in vivo* and affect the relative distribution of Aβ species over toxic and non-toxic conformations over time. Given the complexity of the biophysical environment in which Aβ aggregation occurs *in vivo*, such question is extremely difficult to address. Nevertheless, it is possible to analyse the dynamic features of this process in simplified and controlled conditions *in vitro*, and to evaluate the effect of the relative concentrations of $A\beta_{40}$ and $A\beta_{42}$ to the generation of neurotoxic species over time.

We hypothesized here that the early onset of AD by APP and/or presenilin mutations that increase the $A\beta_{42}$:$A\beta_{40}$ ratios can be explained by interactions between $A\beta_{40}$ and $A\beta_{42}$, which provide stability to intermediate, neurotoxic species. We used biophysical methods and a novel cellular assay to analyse the establishment of neurotoxicity over time in different Aβ mixtures. We found that very minor changes in the relative amount of $A\beta_{42}$ versus $A\beta_{40}$ ($A\beta_{42}$:$A\beta_{40}$) has dramatic effects on the dynamic behaviour of toxic Aβ species. Our findings provide an important biological addition to the original '$A\beta_{42}$ seeding hypothesis' (Jarrett and Lansbury, 1993), which focused on amyloid fibril formation. These dynamic oligomeric species exhibit initial synaptotoxicity and cause later neurotoxicity in primary hippocampal neurons and affect memory formation in mice, underlining their potential importance for the understanding of AD.

Results

As the objective of this study was to investigate how $A\beta_{40}$ and $A\beta_{42}$ affect each others' biophysical and biological properties, it was important to prepare a pre-aggregate-free Aβ solution and to validate the mixtures using mass spectrometry (Supplementary Figure) and anti-$A\beta_{40}$- and anti-$A\beta_{42}$-specific antibodies (Supplementary Figure 1E). We found that the sequential treatment of 1,1,1,3,3,3-hexafluor-2-propanol (HFIP)-Aβ films (rPeptide) with HFIP, dimethyl sulphoxide (DMSO) and then removal of DMSO using a desalting column provide excellent results with mixtures of primarily monomeric peptides in the appropriate relative amounts (Supplementary Figure 1, see also Materials and methods). Fourier transform infrared (FTIR) spectroscopy validated the complete removal of all HFIP and DMSO (not shown).

Aggregation rate of Aβ peptides is strongly influenced by the ratio $A\beta_{42}$:$A\beta_{40}$

Aβ peptide was incubated at a concentration of 50 μM in 50 mM Tris–HCl, 1 mM EDTA, pH 7.5 at 25°C. The aggregation process of a range of $A\beta_{42}$:$A\beta_{40}$ ratios (10:0 to 0:10) tested by Thioflavin T (ThT) fluorescence yielded a typical sigmoidal curve as generally observed for aggregating proteins and peptides (Figure 1A shows four examples) (Harper and Lansbury, 1997). The formation of an Aβ nucleus, which is not reactive with the fluorescent ThT probe during the so-called 'lag phase', is followed by rapid elongation of ThT-positive Aβ aggregates to form fibrils (the 'elongation phase'). Both the length of the lag phase and the rate of aggregation were affected by the ratio of $A\beta_{42}$:$A\beta_{40}$ (Figure 1B and C). The lag phase for pure $A\beta_{40}$ alone was $\sim$2.5 h ($\pm$0.3 h). Addition of 10% $A\beta_{42}$ ($A\beta_{42}$:$A\beta_{40}$ = 1:9) resulted in a small, but reproducible increase in the lag phase ($\sim 2.9 \pm 0.3$ h) (Figure 1B). A further increase in the $A\beta_{42}$:$A\beta_{40}$ ratio decreased paradoxically the length of the lag phase to $\sim 0.5 \pm 0.01$ h. From a ratio of 3:7 onwards, no difference was observed compared with $A\beta_{42}$ alone. The elongation rate was fastest for pure $A\beta_{40}$ and was slowed down by addition of $A\beta_{42}$ (Figure 1C). Remarkably, judging from the lag phase of aggregation, the 1:9 and the 3:7 ratio showed two opposite ends of the spectrum (Figure 1B). These ratios, in addition to 10:0 and 0:10 were selected for our further studies. The choice for 3:7 can be also rationalized as it reflects roughly the ratio of $A\beta_{42}$ and $A\beta_{40}$ in patients with familial AD (Duff *et al*, 1996; Mann *et al*, 1996; Scheuner *et al*, 1996; Citron *et al*, 1997). Thus, both time and the $A\beta_{42}$:$A\beta_{40}$ ratios are two important parameters when considering the biophysical properties of Aβ, and we decided to investigate how these parameters determine Aβ-oligomer toxicity. We describe in the rest of the paper the different Aβ mixtures as an $A\beta_{42}$:$A\beta_{40}$ ratio, incubated for an indicated time at an Aβ concentration of 100 μM in 50 mM Tris–HCl, 1 mM EDTA, pH 7.5 at 25°C. Thus, (3:7, 2 h) means a ratio of three $A\beta_{42}$ versus seven $A\beta_{40}$ peptides incubated for 2 h under

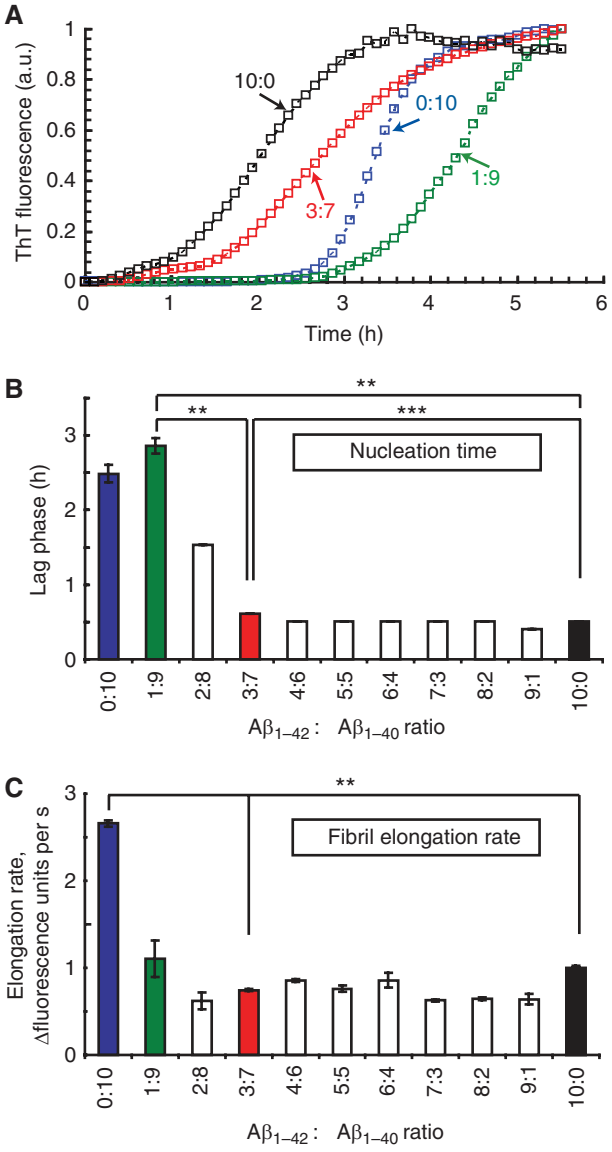

Figure 1 $A\beta_{42}$ determines the kinetics of Aβ aggregation. (**A**) Aggregation kinetics of 50 μM Aβ ratios in 50 mM Tris, 1 mM EDTA at 25°C for 6 h by Thioflavin T (ThT) assay shows how the ratio of $A\beta_{42}$:$A\beta_{40}$ (e.g. 3:7) influences the aggregation kinetics. The colour codes are maintained in all following figures. (**B**) Quantitative analysis of lag phase, showing the time (hours) of the initial part of curves as in (**A**), during which no increase in ThT fluorescence signal is detected using different $A\beta_{42}$:$A\beta_{40}$ ratios as indicated. (**C**) Quantitative analysis of the elongation rate, derived from (**A**) as rate of fluorescence change, which is the slope of the linear phase of exponential growth in (**A**), using different Aβ ratios as indicated. Numbers are averages of three independent experiments. Error flags indicate s.d. calculated over the three independent experiments. Statistical significance of the results was established by *P*-values using paired two-tailed *t*-tests, and only shown for the four ratios further studied in the text. Statistical significance levels were in (**B**, **C**): $*P<0.005$, $**P<0.001$, $***P<0.0001$. *P*-value of $A\beta_{40}$ (0:10) and (1:9) = 0.09, and *P*-value of $A\beta_{40}$ (0:10) and (1:9) = 0.0058 in panels **B** and **C**, respectively.

given buffer conditions before addition to the cell culture. Final concentration of Aβ in cell culture is in most experiments 1 μM apart from a few in which 10 μM was used as indicated. On the basis of our further experiments, it appeared that at any time point only a small fraction of the peptides is in a toxic active conformation.

The $A\beta_{42}$:$A\beta_{40}$ ratio is a driver of acute synaptic alterations

One problem with Aβ toxicity assays is the delay between the actual preparation of the oligomer samples used for the biophysical analysis and the moment when the biological read out becomes available to assess the neurotoxicity. We, therefore, sought to set up an assay that allows verifying biological effects of Aβ preparations within the time frame of the biophysical experiments. We plated mouse hippocampal neurons on *m*icro*e*lectrode *a*rray (MEA)-based chips (Figure 2A) (Stett *et al*, 2003) and recorded spontaneous firing rates in the neuronal networks before and after treatment with Aβ mixtures at a final concentration of 1 μM. Representative traces of responses of cultures treated with different Aβ mixtures are displayed in Figure 2B. Interestingly, treatment with pure $A\beta_{40}$ mixtures (0:10, 2 h) appeared to enhance synaptic activity measured as spontaneous firing rate, whereas (1:9, 2 h) mixtures had no effect on spontaneous synaptic activity (Figure 2B and C). In contrast, $A\beta_{42}$ alone (10:0, 2 h) or with $A\beta_{40}$ (3:7, 2 h) readily suppressed spontaneous neuronal activity within 40 min after addition of the peptides (Figure 2B and C). As a control of the oligomers species status during the course of the recording, we followed changes in fluorescent ThT emission over 40 min of Aβ mixtures at 1 μM in neuronal culture medium at 37°C, which mimics the conditions of the cell culture experiments (Figure 2D). The Aβ mixtures appeared stable over the time frame of the experiment at least as far as it concerns ThT incorporation. We next assayed how different $A\beta_{42}$:$A\beta_{40}$ ratios evolve over time with regard to synaptotoxic properties. $A\beta_{42}$:$A\beta_{40}$ ratio mixtures were incubated for 0, 1.5, 4, 6 and 20 h before addition to the cultures. Synaptic firing rates were recorded for 40 min as above using MEA. Figure 2E shows that synaptic effects were little after treatment of the cells with mixtures of Aβ shortly after dissolving them in buffer ($t = 0$ h, Figure 2E). Toxicity was, however, already significantly high after 1.5 h of aggregation in the (3:7, 1.5 h) and the (10:0, 1.5 h) mixtures. The synaptotoxic potential in the (3:7) and (10:0) ratios remained stable up to 20 h (Figure 2E). Remarkably, 1:9 or 0:10 ratios did not result in major synaptic effects at any incubation point (Figure 2E). To validate the findings, we performed double immunostaining for the synaptic marker synaptophysin and Aβ oligomers using the A11 antibody (Kayed *et al*, 2003). Figure 2F shows that Aβ (3:7) and Aβ (10:0) mainly co-localized with the synaptic marker, whereas staining was not observed with the (1:9) and (0:10) ratio. Extensive washing of the neurons to remove Aβ species did not interfere with consecutive A11 staining, indicating the rather irreversible nature of the binding of these synaptic active species to the neurons (not shown).

To prove Aβ specificity of the observed effects, we pre-incubated cells with anti-oligomer A11 or anti-Aβ antibody 6E10 before treatment with Aβ (10:0, 2 h) ratio. The alterations in the synaptic activity by toxic intermediates are indeed Aβ specific, as cells pre-incubated with antibodies are no longer susceptible to the neurotoxic effects (Figure 2G). We also further explored the reversibility of these Aβ effects on synaptic function. Removal of Aβ (3:7,

2 h) and Aβ (10:0, 2 h) after 40 min of incubation on the neuronal cultures by extensive washes with medium did not restore synaptic activity over the next 6 h in line with the immunofluorescence data (Figure 2H). However, 18 h after the wash out of Aβ (3:7, 2 h) and Aβ (10:0, 2 h), we found partial synaptic activity recovery at some electrodes, although the profile of the action potentials (APs) displayed a slightly different character than the ones recorded before the treatment (Figure 2H). Given the long time needed for some recovery and the fact that the profiles after recovery were different from those before, it seems likely that this partial restoration of neuronal activity is due to the generation of novel synaptic contacts rather than recovery of existing synapses.

In an alternative paradigm to validate the MEA measurements and to evaluate the effect of Aβ on the postsynaptic response only, we performed patch-clamp experiments on 2-week-old neurons and recorded spontaneous electrical activity comprising APs and excitatory postsynaptic potentials (EPSPs) (Figure 3). The effects of Aβ addition were already observed after a few minutes (Hartley *et al*, 1999) and the changes in APs and EPSPs frequency were, therefore, assessed at 7 min and compared with the APs and EPSPs frequency measured during 1 min before Aβ was applied (time point '−1 min'). It is clear that the Aβ (3:7, 2 h) has a profound effect on the EPSP frequency, indicating a block of spontaneous postsynaptic depolarizations Neither APs nor EPSPs were affected by Aβ (1:9, 2 h), and significant increase in APs rate was observed in case of Aβ (0:10, 2 h), in line with the MEA data. As it can be seen, synaptotoxic signatures of Aβ42:40 ratios are similar regardless of extra- or intracellular mode of measurement.

Toxic Aβ species are oligomeric and dynamic structures

We used transmission electron microscopy (TEM) to characterize the morphology of the species populated during fibril formation. At the starting point of incubation, no fibrils are detected with any of the different Aβ ratios (Figure 4A, column 0 h). With time, the pure $A\beta_{42}$ (10:0) solution showed mature fibril formation consistent with the fast nucleation observed by ThT fluorescence. The fibrils have typical long, negatively stained amyloid fibril morphology as is frequently observed for other amyloid-forming proteins or peptides (Chamberlain *et al*, 2000). Upon longer incubation, these fibrils progressively transform into a dense network of clustered fibrils. $A\beta_{42}$:$A\beta_{40}$ (0:10) and (1:9) ratios developed fibrils after ∼6 h, which have similar characteristics to the fibrils observed in the (10:0) ratio, but display in addition a regular twist pattern, which is not observed in the $A\beta_{42}$ fibrils (Figure 4A, most right column, arrows indicate twist pattern). The (3:7) ratio in contrast showed no fibrils at this time point, and the first aggregates appeared only after ∼9 h. These aggregates differed markedly in their morphologies as they interacted heavily with the uranyl acetate stain used to visualize the aggregates in TEM and also formed densely fibrous and fractured networks in which individual fibrils cannot be distinguished, which is similar to the later stages of $A\beta_{42}$ aggregation (not shown). Interestingly, the fast nucleation and aggregation kinetics of the (3:7) ratio as observed using ThT fluorescence assays (Figure 1) did not coincide with the early appearance of mature aggregates using electron microscopy (Figure 4A). This suggested that the (3:7) ratio rapidly generates small ThT-positive oligomers, but that these do not propagate towards assemblies that are sufficiently large to allow visualization with EM. Although EM experiments confirmed clearly the dramatic differences in the aggregation properties of the different mixtures, they did not allow visualizing the postulated toxic species responsible for the synaptic effects observed in the MEA experiments with the (3:7) ratio. We hence set out to further identify the presence of smaller oligomeric Aβ using the complementary technique of tapping mode atomic force microscopy (AFM). The various Aβ ratios under investigation were screened at 1.5 h incubation, which is a time point that yields strong synaptotoxicity for ratios (3:7) and (10:0), but not for ratios (1:9) and (0:10) (Figure 2E). Interestingly, we observed oligomer formation for all four ratios of $A\beta_{42}$:$A\beta_{40}$ (Figure 4B), even for the two non-synaptotoxic ratios (1:9) and (0:10). This finding implies that oligomer formation *per se* is not directly linked to the toxic effects of Aβ. We infer that the internal organization of the oligomers might make them toxic to neuronal cells. Native PAGE showed that (10:0) and (3:7) already display a wide range of oligomers and fibrillar material that did not enter the gel after 4 h incubation. SDS–PAGE in contrast shows at the same time points only low-molecular weight oligomers (Supplementary Figure S2). It, therefore, seems that SDS–PAGE dissociates the larger native structures in the toxic mixtures. The smaller oligomeric SDS-resistant structures can only be considered 'building blocks' of larger toxic structures. As no clear differences were observed in oligomerization state between the four different ratios that could explain the variation in cytotoxicity, we used *in situ* FTIR spectroscopy to obtain information on the conformation of the Aβ peptides and aggregates in solution. We found that the initial spectra of the different Aβ mixtures at $t = 0$, when peptides are mainly monomeric, are characterized by a broad peak at 1654 cm^{-1} indicative of random coil structure (Goormaghtigh *et al*, 1994). This spectrum gradually converts into a defined and sharper peak at 1627 cm^{-1} (Figure 5). The intensity at 1627 cm^{-1} is indicative for β-sheet-organized aggregates (Chirgadze and Nevskaya, 1976) and the concomitant increases of the FTIR signal at 1627 cm^{-1} with a decreased signal at 1654 cm^{-1} suggested a transition from disordered monomeric structures to β-sheet enriched-oligomeric structures in all mixtures (Figure 5, panels A–D). Conformational changes are rapidly evolving for the three Aβ ratios that contain $A\beta_{42}$, but the rate of this change does not seem to predict toxicity: $A\beta_{42}$ is toxic at 1.5 h, whereas ratio 1:9 is not. For $A\beta_{40}$ alone (Figure 5A) and for Aβ (1:9) (Figure 5B), it appears that the loss of unordered structure (1654 cm^{-1}) coincided with a prompt transition into amyloid fibrillar β-sheet structure (1627 cm^{-1}), suggesting a two-state manner in the mixtures that develop at inverse rates. This is not observed for Aβ (3:7) and Aβ (10:0), suggesting that there is an intermediate, which seems to be correlated with toxicity.

Long-term cellular toxicity of Aβ mixtures

Although the changes in synaptic activity are clearly an early effect of the toxic conformations in the Aβ preparations, it remained unclear whether these initial hits on the synapse could also evolve to full cellular neurotoxicity. This is an important question with regard to AD as the disease is characterized in essence by neuronal cell loss. We

investigated, therefore, the effects of the different $A\beta_{42}$:$A\beta_{40}$ ratios over two distinct concentrations (1 μM, which appeared sub-lethal and 10 μM, which appeared lethal) on the staining pattern of primary hippocampal neurons with the synaptic marker synaptophysin or with the early apoptotic markers cleaved caspase-3 and annexinV/propidium iodide (PI). Treatment of cells with 1 μM concentration of Aβ ratios (the same as used for the MEA experiments) for 12 h clearly decreased synaptophysin staining for the Aβ (3:7, 2 h) and Aβ (10:0, 2 h) ratios. At this concentration, no or little effect on appearance of apoptotic markers in the neuronal cells was observed (Figure 6A; quantified in Figure 6C), further indicating that the initial effect of the Aβ toxic intermediates is at the synapses. However, 10-fold higher concentration of Aβ

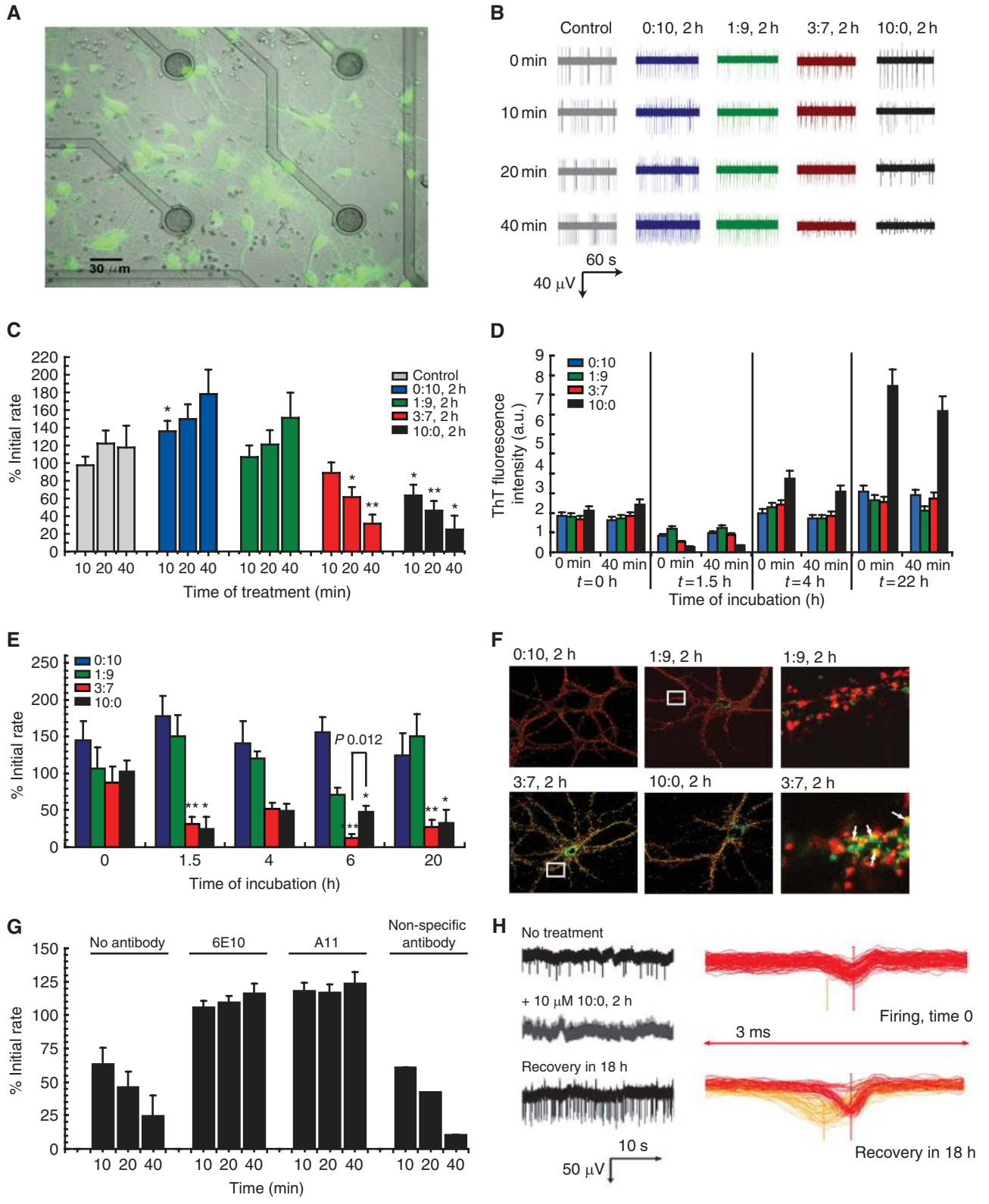

(3:7, 2 h) and Aβ (10:0, 2 h) ratios resulted not only in the loss of synaptophysin staining, but was accompanied by a strong increase in the early apoptotic markers, annexin V/PI and cleaved caspase-3 staining (Figure 6B; quantified in Figure 6D). In contrast, synapses remained intact and no early apoptotic marker induction was caused by Aβ (0:10, 2 h) and Aβ (1:9, 2 h) ratios at both 1 and 10 μM concentrations after 12 h of treatment (Figure 6C and D). This finding indicates that synaptotoxic and cytotoxic effects of Aβ intermediates are both ratio and concentration dependent.

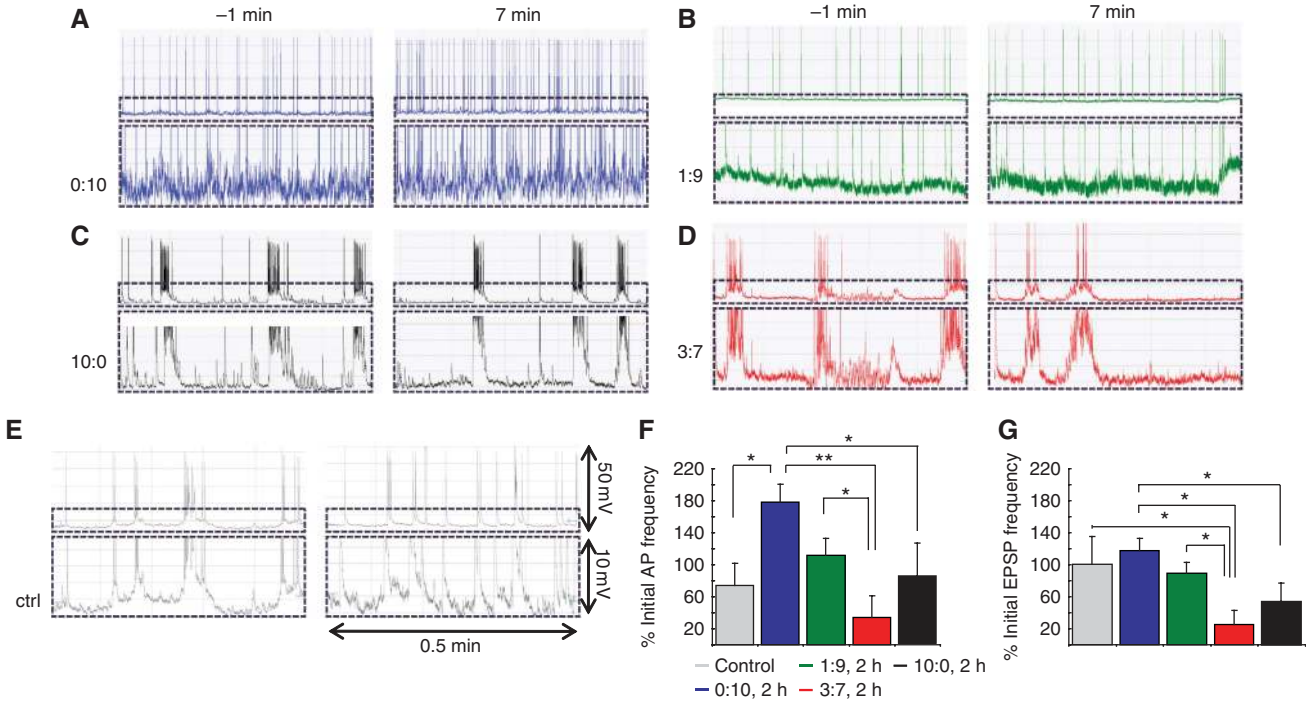

Figure 3 Patch-clamp measurements in primary cultures of neurons. (**A–D**) Firing pattern of spontaneously active patch-clamped neurons 1 min before and 7 min after the treatment with different Aβ ratios (2 h) as indicated. (**E**) Measurement in control conditions (only buffer) (**F**) Relative changes in spontaneous action potentials (AP) frequency expressed as per cent of initial (−1 min) rate. Note the early increase in AP rate for $Aβ_{40}$ (0:10)-treated neurons. The other ratios do not reach statistical significance as compared with control likely because of the comparatively short time of treatment. (**G**) Relative change in single excitatory postsynaptic potentials (EPSP). Note the significantly decreased EPSPs rate for $Aβ_{42}$:$Aβ_{40}$ ratio 3:7 ($P<0.03$ versus control, unpaired two-tailed *t*-test) after only 7 min of treatment. Values are per cent of initial firing rate ± s.e.m. of at least three independent experiments. Statistical significance of the data is indicated by $*P<0.035$ or $**P<0.01$ in (**F**) and (**G**).

Figure 2 Mixed Aβ oligomers result in a rapid synaptotoxic response in primary neurons. (**A**) Neurons stained with Fluo-4 were cultured 8 days *in vitro* (DIV) on the MEA chip. (**B**) Firing pattern of neurons from representative electrodes at 0, 10, 20 and 40 min treatment with different Aβ ratios prepared as indicated (e.g. 0:10, 2 h means an $Aβ_{42}$:$Aβ_{40}$ ratio of 0 versus 10, and 2 h means 2 h incubation before addition to the culture). Note the significantly decreased firing rate and amplitude for $Aβ_{42}$:$Aβ_{40}$ ratios 10:0 and 3:7 after 20 min of treatment. (**C**) Spontaneous electrical synaptic activity recordings of hippocampal neurons during 40 min of treatment with 1 μM Aβ ratios incubated for 2 h prior to the addition to cells. Values are per cent of initial firing rate ± s.e.m. of 3–5 independent experiments. Statistical significance (unpaired two-tailed *t*-test) of the data versus control is indicated by $*P<0.01$ or $**P<0.001$ in the figure. Notice that a strong reduction in spontaneous synaptic firing versus correspondent control (buffer-treated chips) can be observed after 20 and 40 min in the medium of the 3:7 and 10:0 $Aβ_{42}$:$Aβ_{40}$ ratios. (**D**) Oligomers dissolved in culture medium remain stable with regard to ThT tinctorial properties for at least 40 min. Aβ ratios were prepared and at specific time intervals of incubation, that is 0, 1.5, 4 and 22 h, Aβ aliquots were removed and diluted to 1 μM in cell culture medium containing ThT. The stability of the aggregates at 37°C in cell culture medium was deduced from the stability of the ThT signal over 40 min. Blue bars represent different $Aβ_{42}$:$Aβ_{40}$ ratios as indicated in the figure. Compare signals directly upon dilution into cell culture medium ('0 min') at 37°C with signals obtained after 40 min incubation at 37°C ('40 min'). Values are averages of three experiments. (**E**) Different ratios of Aβ peptides were generated and added to neuronal cultures diluted to a final concentration of 1 μM, either immediately (0 h) or after 1.5 h; 4 h, 6 h or 20 h of incubation. Synaptotoxicity was measured by recording a decreased rate of firing 40 min after adding the Aβ mixtures to the neurons. Statistical significance levels determined as a function of s.e.m.: $***P<0.0001$, $n=6$ chips, $**P<0.001$, $n=3$ chips, $*P<0.01$, $n=3$ chips, difference between 6 h ratio (3:7) and (10:0): $*P<0.012$ (unpaired two-tailed *t*-test). (**F**) Synaptic localization of mixed Aβ oligomers. Fluorescence microscopy images of hippocampal neurons stained for synaptophysin (red) and Aβ oligomers (A11 antibody) (green) after 1 h treatment with 1 μM of the indicated Aβ ratios, incubated for 2 h prior the addition to cells. Right panel: magnification of selected region stained with synaptophysin (red) and Aβ oligomers (A11 antibody, green). Oligomeric Aβ co-localizes with synapses. (**G**) Rescue of spontaneous electrical synaptic activity after the treatment with ratio (10:0, 2 h) in the presence or absence of anti-oligomer A11 or anti-Aβ 6E10 antibody, final concentration 10 μg ml^{-1}. Values are per cent of initial firing rate ± s.e.m., of three independent experiments, except for the control with non-specific antibody, which was performed only once. (**H**) Example of firing recovery after treatment with 10 μM (10:0, 2 h). Raw data streams are shown in black, and corresponding spike shapes are in red. The treatment completely inhibited spontaneous activity in 6 min. Then the medium was refreshed, and signals were measured after overnight recovery (18 h). Note partial restoration of initial firing profile along with appearance of another spike population endowed with slightly different waveform and amplitude. Spike sorting is performed in MC Rack software.

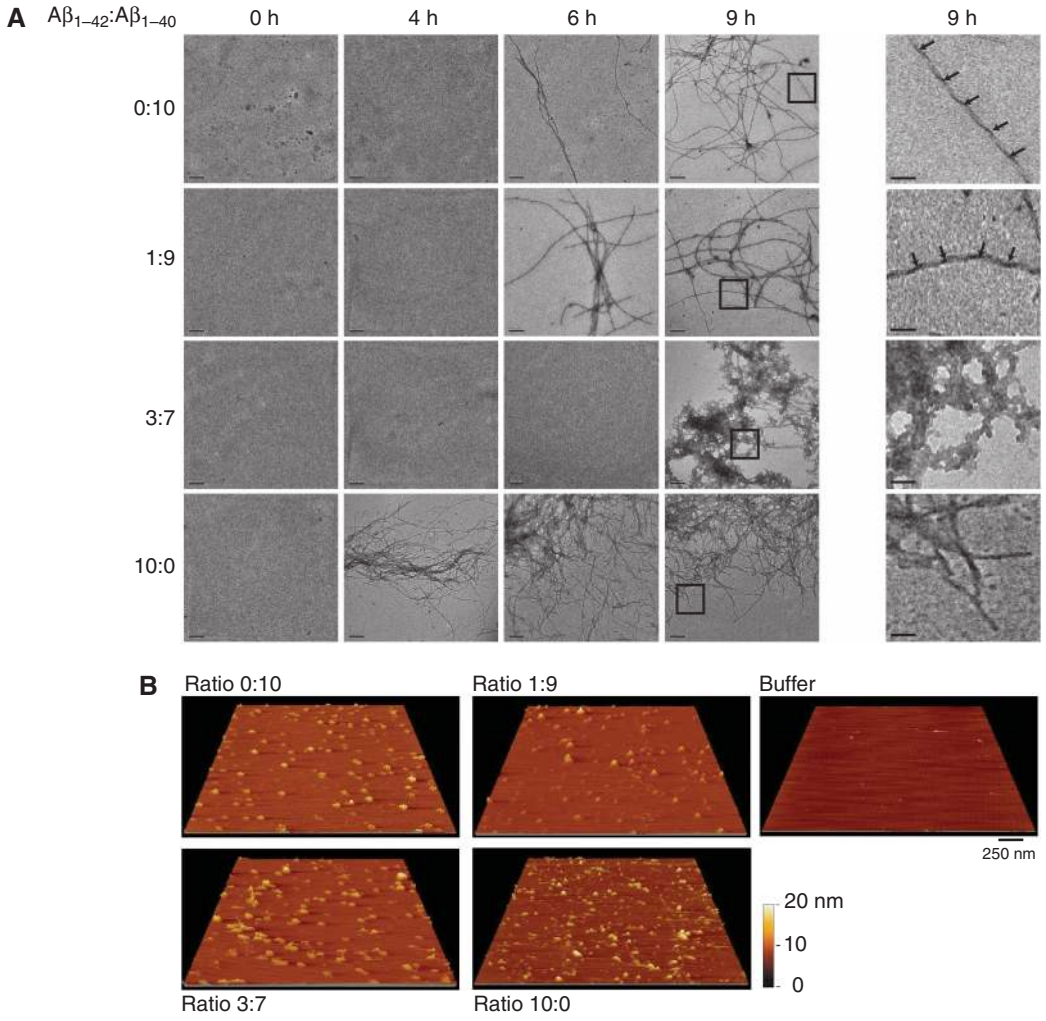

Figure 4 Characterization of Aβ oligomers with transmission electron microscopy and atomic force microscopy. (**A**) Transmission electron microscopy images of Aβ ratios incubated for 0, 4, 6 and 9 h. Images shown are representative for two experiments. Time of appearance and fibril morphology are affected by $A\beta_{42}$:$A\beta_{40}$ ratio and mature fibril formation is delayed for the synaptotoxic 3:7 ratio. The bars represent 0.2 μm size. The last column shows a magnification of the area indicated by squares in the panels of 9 h. The bars represent 0.04 μm size. The arrows indicate a regular twist pattern observed in the 1:9 and 0:10 fibrils. (**B**) AFM height images of Aβ oligomers formed by incubation of 70 μM Aβ for 1.5 h at 25°C in 50 mM Tris, 1 mM EDTA. The buffer image is shown as a control. The bar represents 250 nm size.

We evaluated the time course of caspase-3 activation and its sub-cellular localization versus the synaptic marker synaptophysin in both sub-lethal (1 μM) and lethal (10 μM) concentrations of the (3:7, 2 h) ratio (Figure 6E). Cells treated with 1 μM (3:7, 2 h) showed that cleaved caspase-3 after 2 and 6 h was mostly observed in areas positive for synaptophysin staining. Further treatment up to 12 h resulted in loss of synapses as indicated by loss of staining for synaptophysin; however, the cleaved caspase-3 immunostaining did not propagate to the soma and nucleus. Treatment with 10 μM (3:7, 2 h) caused in contrast strong activation of caspase-3 at the synapses already after 2 h (Figure 6E). In addition, immunostaining for activated caspase-3 was clearly detectable after 6 h in the soma of the cells. At 12 h, this concentration resulted in loss of synaptic staining with synaptophysin antibodies and strong staining of activated caspase-3 in the soma and nucleus indicative of cell apoptosis (Figure 6E). A similar pattern was detected with (10:0, 2 h), but not for (0:10, 2 h) or (1:9, 2 h) (not shown). These data indicate that the Aβ toxicity observed at the level of the synapses can spread towards the cell body depending on the type of Aβ species and concentration of toxic intermediates. In addition, the observation suggests that synapse toxicity and cellular toxicity are related.

To further confirm that the different Aβ preparations exerted cellular toxicity, we used a Cell-Titer Blue viability assay on neurons 48 h after they had been exposed to 10 μM of different Aβ ratios, taken at the start of the aggregation process (0 h in Figure 6F) and during the propagation reaction (1, 2, 4 and 12 h in Figure 6F). In agreement with the previous studies, monomers (Figure 6F, 0 h) and mature fibril preparations (Figure 6, 12 h) are largely inert towards neurons (Aksenov *et al*, 1996; Martins *et al*, 2008). In contrast, the $A\beta_{42}$:$A\beta_{40}$ (3:7, 1 and 2 h) and (10:0, 1 and 2 h) exhibited clear neurotoxicity (Figure 6F). Both (1:9) and (0:10) did not exhibit neurotoxicity at any stage of the aggregation process (Figure 6F). Collectively, these data indicate that stabilized intermediates in the Aβ (10:0) and (3:7) ratios bind to synapses and inhibit synaptic activity, and affect neuronal viability at higher concentrations.

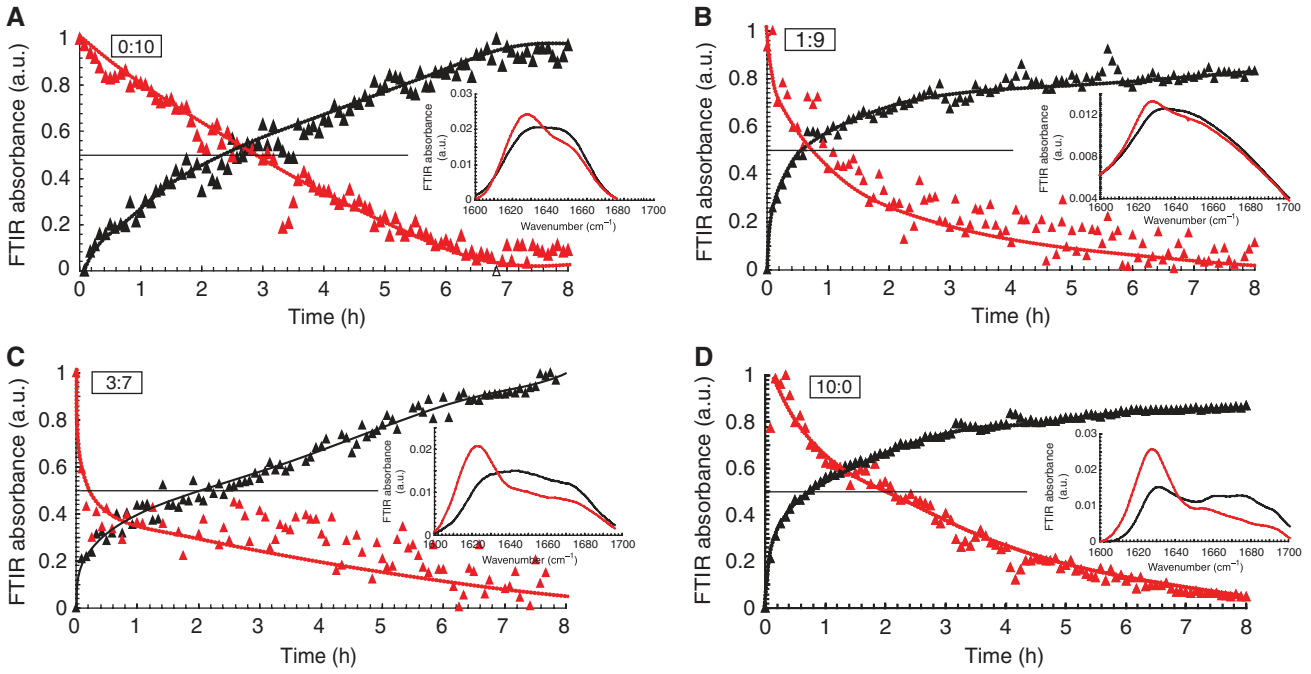

Figure 5 Conformational transitions observed using Fourier transform infrared (FTIR) spectroscopy. FTIR spectra were collected continuously upon incubation of Aβ ratios at 25°C to investigate conformational changes over time. (**A**) $A\beta_{42}$:$A\beta_{40}$ (0:10), (**B**) $A\beta_{42}$:$A\beta_{40}$ (1:9), (**C**): $A\beta_{42}$:$A\beta_{40}$ (3:7) and (**D**) $A\beta_{42}$:$A\beta_{40}$ (10:0). Intensity at 1654 cm^{-1} in red characteristic for disordered structure (▲) and intensity at 1627 cm^{-1} in black (▲) characteristic for amyloid fibril structure. Intensities are averages of three independent experiments and normalized against buffer. Notice that the transition of ratio (3:7) and (10:0) cannot be explained by a two-state transition model (the two curves do not cross at the 50% intersection), whereas (0:10) and (1:9) can completely be accounted for by the two states. Insets show typical spectra for the different Aβ ratios recorded at 0 h (black) and after incubation for 8 h (red).

Aβ ratio affects behaviour and learning alteration in mice

We finally evaluated to what extent the different Aβ ratio mixtures affected memory formation in mice *in vivo*. We injected mice intraventricularly with 6 μl of 100 μM Aβ mixtures allowed to aggregate for 1.5 h before the injection. The effect of these Aβ preparations on memory formation was tested using passive avoidance and contextual/auditory-cue fear conditioning as described previously (Martins *et al*, 2008). In a light–dark step-through task (passive avoidance test), animals were trained to memorize an electrical shock that followed entrance to a dark compartment. When the test was repeated 24 h later, animals injected with (0:10, 1.5 h) or (1:9, 1.5 h) recalled the electroshock correctly and showed a latency to enter the dark room of 232 ± 15 and 273 ± 16 s, respectively, which was not significantly different from control mice injected with buffer (256 ± 20 s)-control group not shown. Injection of (10:0, 1.5 h) or (3:7, 1.5 h) before the shock, however, inhibited strongly the formation of new memory. These animals showed significantly faster entrance latencies of 134 ± 12 and 165 ± 19 s, respectively ($P<0.002$) (Figure 7A). Contextual and auditory-cue fear conditioning experiments confirmed these results. Injection of (10:0) and (3:7) 90 min before conditioning disturbed the typical freezing behaviour observed 24 h after the training when the animals were exposed again to the contextual stimulus (~50%, $P<0.006$) or the auditory-cue fear conditioning experiment (39%, $P<0.004$) (Figure 7B). These results show that also in the complex environment of a living animal clear differences can be observed between the different Aβ ratios similar to those observed in biophysical and cellular assays.

Discussion

One of the most challenging issues in AD research is the unresolved nature of the Aβ-peptide conformation(s) that exert neurotoxicity. Our current work shows that Aβ-associated toxicity is a dynamic property and that a critical equilibrium between the two major Aβ species, $A\beta_{40}$ and $A\beta_{42}$, exists, which determines the rate of appearance of these toxic properties as assessed in neuronal cell culture and in brains of animals *in vivo*. Our study design has taken this dynamic behaviour into account by indicating the time of aggregation of the peptides used in each experiment. We found that relative high concentrations of Aβ are needed to induce fibrillization and toxic-oligomer conformation. Although this might seem an artificial situation, one should realize that by increasing the Aβ concentrations, processes which otherwise take decades become accelerated to the extent that they can be studied in laboratory conditions. Most importantly, such high concentrations of Aβ might actually be even quite relevant for what happens *in vivo*. A recent publication suggested indeed that intracellular compartments accumulate Aβ at high μM concentrations, which could create the conditions for the local formation of the elusive toxic conformations of Aβ peptides (Hu *et al*, 2009).

It turns out that a small relative increase of $A\beta_{42}$, comparable with those observed in patients with familial cases of AD

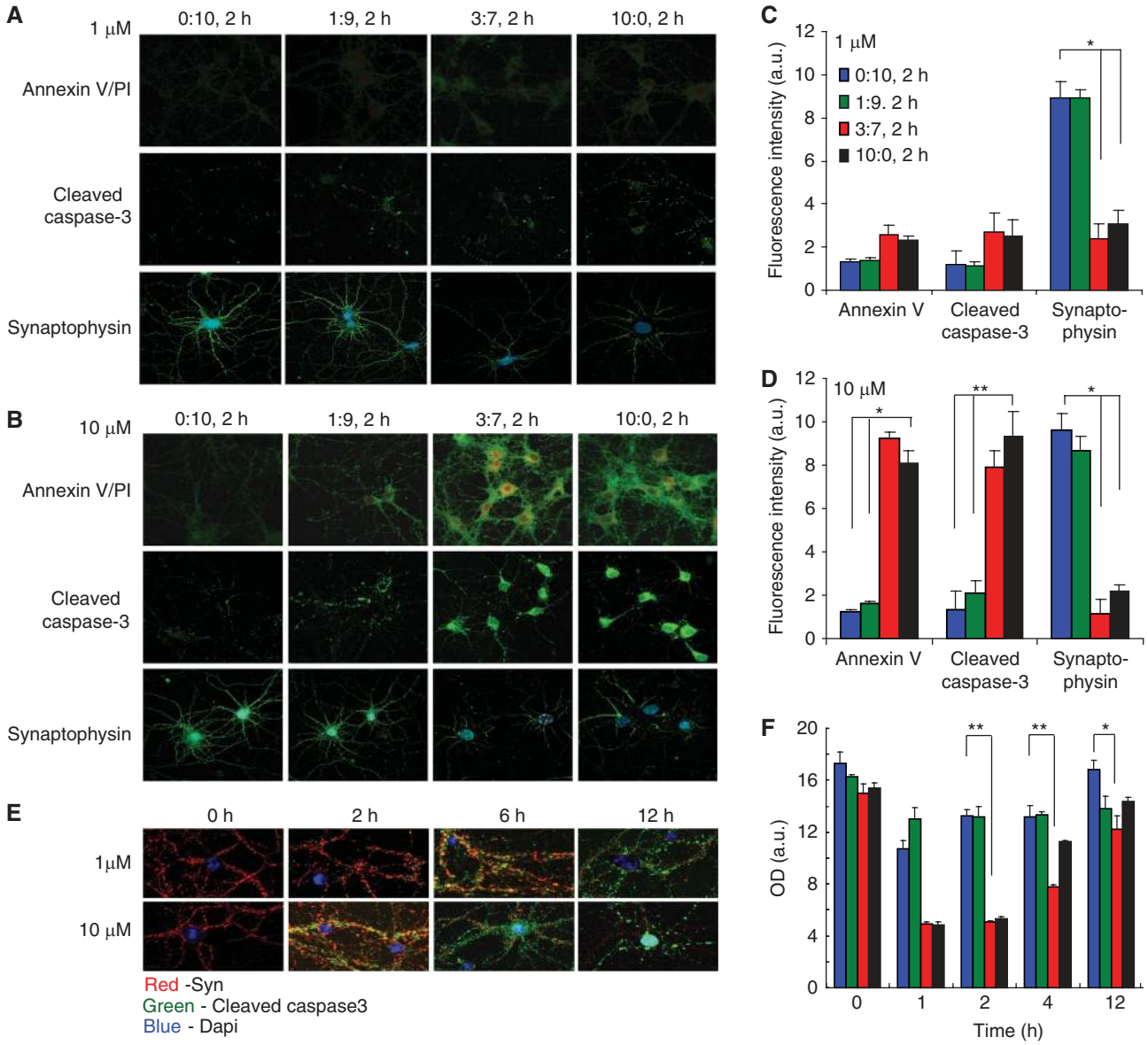

Figure 6 Mixed Aβ oligomers affect synapses at low concentration and induce cell death at higher concentrations. (**A**, **B**) Fluorescence microscopy images of hippocampal neurons stained for annexin V (green)/PI (red) (upper row), cleaved caspase-3 (middle row) and synaptophysin (green)/DAPI (blue) (bottom row) after 12 h treatment with (**A**) 1 μM Aβ ratios and (**B**) 10 μM Aβ ratios incubated for 2 h before the addition to cells. Fluorescence intensity quantification for annexin V, cleaved caspase-3 and synaptophysin staining (**C**) 1 μM and (**D**) 10 μM of Aβ ratios. Values are intensity ± s.e.m., $^{**}P<0.001$ and $^{*}P<0.003$, of five different areas from two independent experiments. (**E**) Time course of fluorescence microscopy study of hippocampal neurons stained for synaptophysin (red) and cleaved caspase-3 (green) after treatment with 1 and 10 μM 3:7 ratio Aβ oligomers incubated for 2 h prior the addition to cells (blue: DAPI) figure representative for two independent experiments. (**F**) Cell-Titer Blue viability assay of hippocampal neurons treated with 10 μM Aβ ratios incubated for different time periods before the addition to cells. The Cell-Titer Blue reagent conversion was determined 48 h after the treatment. Values are OD ± s.e.m., $^{**}P<0.01$, three independent experiments performed in triplicates.

(Duff *et al*, 1996; Mann *et al*, 1996; Scheuner *et al*, 1996; Citron *et al*, 1997), dramatically influenced the final effects on spontaneous synaptic activity and viability of neuronal cells and on memory formation in animals. This correlated with remarkable changes in the biophysical behaviour of the Aβ peptides as assessed in a variety of approaches. Thus, we find that shifting the ratio of $Aβ_{42}$:$Aβ_{40}$ from (1:9) to (3:7) shortened nucleation time strongly, whereas fibril elongation time remained similar as measured by ThT incorporation. In EM, the (3:7) ratio revealed only visible fibrillar structures after prolonged incubation compared with the other three ratios investigated. Both experiments together suggested that intermediary assemblies of Aβ peptides became stabilized in the (3:7) ratio, which were too small to be observed in EM, but which, as evaluated in MEA, exerted strong effects on synaptic activity. In SDS–PAGE, these assemblies apparently fall apart in small multimeric Aβ oligomers as observed by others (Walsh *et al*, 2002; Shankar *et al*, 2008), but from non-denaturing PAGE analysis, we deduced that these 'building blocks' are part of larger structures present in the toxic

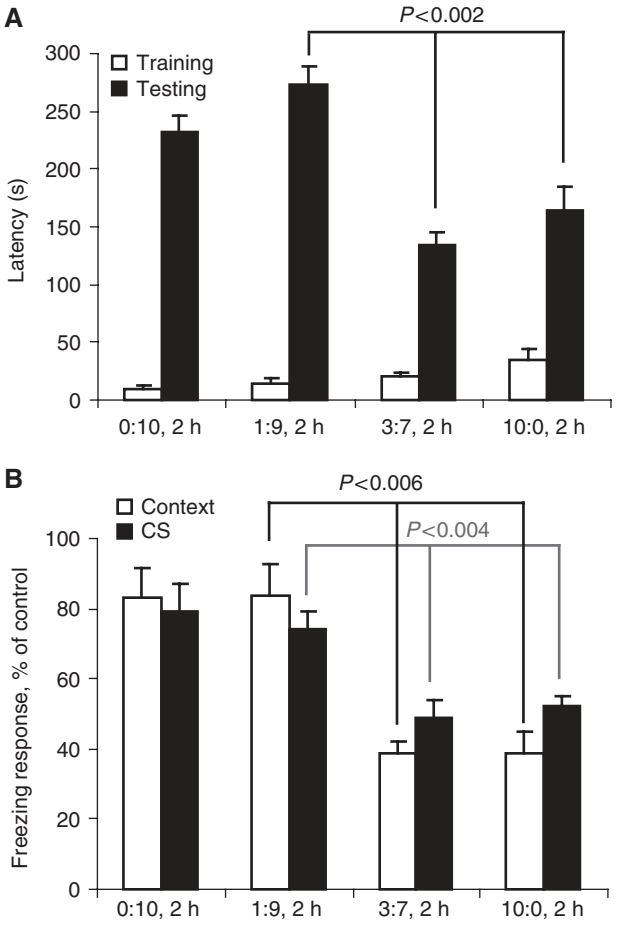

Figure 7 Toxic Aβ affects behaviour and learning of mice. (**A**) Passive avoidance; 1.5 h after intraventricular injection with 6 μl of Aβ ratios incubated for 2 h before the injection, latency of entrance in the dark cage during the training (white) was tested. The latency of entrance during the testing was performed 24 h later (black) (values are latency mean ± s.e.m., $P<0.002$, control ($n=13$), $A\beta_{40}$ and ratio 1:9 ($n=12$), ratio 3:7 and $A\beta_{42}$ ($n=11$)). (**B**) Conditional fear response; 1 h after intraventricular injection with 6 μl of Aβ ratios, habituation was induced. Animals were exposed to the training after an additional 4 h. The freezing response was recorded 24 h later for context-dependent (white bars) and auditory cue-dependent (black bars) memory formation. Values are per cent freezing mean ± s.e.m., Aβ ratios (0:10) and (1:9): $n=13$ for ratio (3:7) and (10:0): $n=14$.

mixtures on the neuronal cultures. Investigation by AFM further underlined that oligomeric Aβ was present in all Aβ ratio preparations, suggesting that the presence of oligomers *per se* are not directly linked with toxic effects. We suggest, therefore, that the toxic aggregates of Aβ in our assays were dynamic in nature and could assemble and disassemble when in solution in the culture medium of the cells. In addition, based on the results obtained by AFM, one can assume that not the size but the structure of the intermediate oligomers dictates their stability and synaptotoxic potential. Indeed, with FTIR spectroscopy, we found indications for particular conformational transitions in the peptides that are specific for this postulated toxic intermediate situation. Going from monomeric Aβ (disordered at 1654 cm^{-1}) to fibrillar Aβ (parallel β-sheet at 1627 cm^{-1}) (Chirgadze and Nevskaya, 1976; Goormaghtigh *et al*, 1994), we find in the $A\beta_{40}$ (0:10) or $A\beta_{42}$:$A\beta_{40}$ (1:9) preparations that the unstructured state converted to the β-sheet conformation without intermediary structures. In contrast, the patterns of conversion in the $A\beta_{42}$:$A\beta_{40}$ (3:7) and the $A\beta_{42}$ (10:0) ratios indicated the existence of an intermediate conformation (Figures 4D and 5C). The current work also suggests the prolonged time window of existence of such intermediate states in the (3:7) ratio.

$A\beta_{42}$ drives apparently this reaction. As shown in Supplementary Figures 3 and 4, interactions of $A\beta_{42}$ and $A\beta_{40}$ occur random (Supplementary Figures 3 and 4). Previously, it has been shown that $A\beta_{42}$ induces indeed the aggregation of $A\beta_{40}$ (Jarrett and Lansbury, 1993; Snyder *et al*, 1994; Yoshiike *et al*, 2003; Yan and Wang, 2007; Jan *et al*, 2008). We show here that the relative amount of $A\beta_{42}$ is most crucial in this regard as shown by the dramatic shift in properties from $A\beta_{42}$:$A\beta_{40}$ ratio (1:9) towards the FAD-like $A\beta_{42}$:$A\beta_{40}$ ratio (3:7). In fact, ratio (1:9) is nucleating very late (Figure 1), but once the nucleation occurs, this mixture rapidly forms mature and well-organized fibrils (Figure 4A), in which oligomer formation is observed by AFM (Figure 4B), but not by TEM. Collectively, the data suggest that the Aβ (1:9) and (0:10) ratios most probably bypassed the synaptotoxic stage and aggregated once nucleation had been induced quite rapidly into non-toxic mature fibrils (Figures 2E–F and 4A) and, therefore, did not bind and affect synapses. In contrary, Aβ (3:7) and Aβ (10:0) ratios were enriched with synaptotoxic intermediates that bind to synapses and inhibit spontaneous synaptic activity. It should be mentioned that it has been already suggested that neurotoxicity by Aβ is not exerted by a specific species, but that in contrast the polymerization reaction itself, which depends on monomer concentration and nucleation rate, drives toxicity (Wogulis *et al*, 2005). Our data seem indeed more compatible with a dynamic interpretation of Aβ toxicity, and argue against a simple receptor-ligand mechanism mediated by a precise Aβ species as has been proposed by several others (e.g. Lauren *et al*, 2009).

A wide range of evidences indicate that Aβ oligomers and protofibrillar intermediates, regardless of their origin or preparation, attack synapses, block LTP and disrupt cognitive functions (Walsh *et al*, 2002; Gong *et al*, 2003; Cleary *et al*, 2005; Calabrese *et al*, 2007; Lacor *et al*, 2007; Martins *et al*, 2008; Tew *et al*, 2008). One of the questions in these assays is whether the species that exerts the toxicity as measured in the biological assay is the same as the one that is analysed in the biophysical assays. We developed, therefore, an acute cellular assay to measure synaptic effects very early after addition of the Aβ preparations. We observed changes in the spontaneous firing rate of neurons in culture already within 20 min incubation with Aβ ratio mixtures (Figure 2D and E). We confirmed that the ThT tinctorial properties of the different Aβ preparations used were minimally changed over the time frame of 40 min. This assay was performed in neuronal culture medium and at the same dilution and temperature used in the cellular assays, further strengthening our assumption that the toxicity measured in the MEA cellular assay was indeed associated with the Aβ aggregation state characterized in the biophysical assays. This acute toxicity was further confirmed by measuring EPSP of neurons in culture: as early as 7 min after addition of the Aβ mixtures toxicity, measured as decreased rate of EPSP, was detected.

We addressed the question of synaptotoxic versus cytotoxic effects of Aβ intermediates. We show that intermediates from the Aβ (3:7) ratio specifically bind synapses (Figure 2F) without major cytotoxicity as assessed by caspase-3 and annexin staining (Figure 6). Our data also provide some preliminary evidence that the initial synaptotoxicity is accompanied by some local synaptic activation of caspase-3 (Figure 6) occurring in parallel to the functional inactivation of synapses (Figure 2), which needs further exploration. Interestingly, higher concentrations of the Aβ(3:7) ratio caused caspase-3 activation in the soma as well (Figure 6).

The findings in the current manuscript impact on our understanding of the function of the different Aβ species and their relative contribution to synapse toxicity and neuronal cell death in the brain of AD patients. The paradox of loss of function of several presenilin mutations causing AD (reviewed in De Strooper, 2007) indicates that at least in these FAD cases, a lower generation of Aβ peptide can still be associated with disease and progressive amyloid accumulation. *In vivo* experiments are in line with this conclusion: more amyloid pathology was observed in transgenic mice expressing a PS1 mutant allele over a PS1 null allele than over a PS1 wild-type allele (Wang *et al*, 2006). Our work explains that it is indeed possible to come to very different, pathologically relevant, situations with the same quantitative Aβ load, but with a qualitatively different Aβ mix. This could potentially explain the early and aggressive neurodegeneration in the brain of presenilin FAD patients, even with a loss of function of γ-secretase (Bentahir *et al*, 2006). If indeed the specific mix of the different Aβ peptides with specific conformation in the brain dictates the synapse and neuronal toxicity potential of the Aβ load in FAD and, by extrapolation, in sporadic AD brain, these observations have obviously important implications for the development of anti-amyloid medication.

Materials and methods

Preparation of Alzheimer's β-peptide ratios

Aβ peptide was dissolved at a concentration of 1 mg ml^{-1} in HFIP (99 + %, Aldrich Cat. # 10,522-8). $A\beta_{42}$ and $A\beta_{40}$ were then mixed in molar ratios of (0:10), (1:9), (3:7) and (10:0). HFIP was evaporated using a gentle stream of argon gas and the peptide film was resolved using DMSO, (Sigma Cat. # D4540) at a final concentration of 1 mg ml^{-1}. The peptide was separated from DMSO with a 5-ml HiTrapTM desalting column (GE Healthcare, Sweden). Complete removal of DMSO was confirmed by FTIR: DMSO provides spectral maxima at 1011 and 951 cm^{-1}. The peptide was eluted into a 50-mM Tris, 1 mM EDTA buffer, pH 7.5 and the peptide concentration was measured using Bradford assay. The samples were kept on ice until experiments started, with a maximum lag time of 20 min.

ThT fluorescence

Aβ protein concentrations were normalized to 50 μM by further dilution using 50 mM Tris, 1 mM EDTA containing buffer and a final concentration of 12 μM ThT was added in a Greiner 96-well plate. The fibrillation kinetics were followed *in situ* using a Fluostar OPTIMA fluorescence plate reader at an excitation wavelength of 440 nm and an emission wavelength of 480 nm. Readings were recorded in triplicate every 10 min for a period of 6 h.

Transmission electron microscopy

Aliquots (5 μl) of the Aβ preparation were adsorbed to carbon-coated FormVar film on 400-mesh copper grids (Plano GmbH, Germany) for 1 min. The grids were blotted, washed twice in droplets of Milli-Q water and stained with 1% (wt/vol) uranyl acetate. Samples were studied with a JEOL JEM-2100 microscope at 200 kV.

Fourier transform infrared spectroscopy

Aβ solutions were applied to the FTIR sample holder and incubated for 8 h at 25°C. InfraRed spectra were recorded on a Bruker Tensor 27 infrared spectrophotometer (Bruker Optik GmbH, Ettlingen, Germany) equipped with a Bio-ATR II accessory. The spectrophotometer was continuously purged with dried air. Spectra were recorded at a spectral resolution of 4 cm^{-1} and 120 accumulations were performed per measurement. FTIR spectra were recorded every 5 min *in situ* at a wavelength range from 900 to 3500 cm^{-1}. The obtained spectra were baseline subtracted and rescaled in the amide I area, which spans from ~1600 to ~1700 cm^{-1}.

Spontaneous synaptic activity recording by MEA

Neurons were plated at 1000 cells mm^{-2} on an MEA substrate (Multichannel Systems GmbH, Germany) and grown for 8–10 days. The spontaneous firing rate of the neuronal network was recorded simultaneously from at least 10 successful electrodes (out of 60 available) (Pine, 1980; Potter and DeMarse, 2001). During the recording experiment, a temperature controller from Multichannel Systems was used to maintain the MEA platform temperature at 37°C. The basal firing rate was recorded during 5 min. Upon treatment with Aβ, the spontaneous synaptic activity was continuously recorded during 40 min. Raw signals from MEA electrodes were amplified by MEA1060 amplifier (gain 1200) from Multichannel Systems and digitized by the A/D MC_Card at a sampling rate of 25 kHz; MC_Rack 3.5.10 software (Multichannel Systems) was used for data recording and processing. The raw data stream was high-pass filtered at 200 Hz, and the threshold for spike detection was set to 5 s.d. of the average noise amplitude computed during the first 1000 ms of recording. A number of spikes detected by every electrode per time bin of 60 s was normalized to baseline (firing rate in the absence of treatment). After data analysis, the firing rates at 10, 20 and 40 min of treatment were extracted and presented as percentage of initial rate.

Patch-clamp experiments

Two-week-old neurons from at least five independent hippocampal cultures were patch clamped, and spontaneous electrical activity comprising APs and EPSPs was recorded. Quartz glass pipettes with an inner diameter of 1 mm were pulled using a P-2000 Laser Puller (Sutter) to obtain pipettes with series resistance of 2–4 MΩ. The pipette solution consisted of 140 mM KCl, 5 mM EGTA, 5 mM NaCl, 5 mM Na_2ATP, 10 mM HEPES, 1 mM $MgCl_2$, pH 7.2. After the formation of a gigaseal, the cell membrane was ruptured using ZAP pulses to obtain the whole-cell configuration. Then, APs and EPSPs were recorded in current clamp mode using a Multiclamp 700B amplifier connected to a Digidata 1440 acquisition card and Clampex 10.2 software (Molecular Devices). Neurons were kept in neurobasal cell medium supplemented with 10% HEPES. Different ratios of Aβ were added to the measurement chamber by manual pipetting. The number of EPSPs before and after the treatment were analysed in 1 min segments by means of the Clampfit software (Molecular Devices).

Learning and memory tests

Passive avoidance learning was tested in a step-through box. During training, dark-adapted mice were placed in the small illuminated compartment of the box. After 5 s, a sliding door to the larger dark compartment was opened, and entry latency was recorded. The door was closed as soon as all four feet were on the grid floor, and a slight foot shock (0.3 mA, 2 s) was delivered using a constant current shocker (Med Associates). Retention was tested 24 h later using the same procedure, and entry was recorded up to 300 s cutoff. The results are expressed as latency to enter the dark compartment before and after the foot shock.

In cue- and context-dependent fear conditioning the unconditioned stimulus (US) (an electric shock) is paired with a CS (the tone) to elicit a freezing response, a reliable measure of fear in rodents. On the first day, the animals were placed in the testing chamber (22.5 × 32.5 × 33.3 cm; Plexiglas cage with a grid floor) and were allowed to acclimatize for 5 min. On day 2, they were first allowed to explore the testing chamber for 2 min (pre-US score). A 30-s tone (conditioned stimulus (CS)) was delivered (frequency, 2150 ± 200 Hz; Star Micronics, Piscataway, NJ), which coterminated

with a 2 s, 0.35 mA foot shock (the US). Two minutes later, a second pairing of the CS and US was presented, followed by another 30 s exploration (post-US score). Twenty-four hours later, the animals were returned to the testing chamber for 5 min exploration in the same context as the previous day (context score). Ninety minutes later, the animals were returned to the test chamber, but now the grid floor was hidden with a Plexiglas plate and odourized sawdust to alter the context of the testing chamber. The animals were observed for 6 min. During the first 3 min, no stimulus was delivered (pre-CS score). During the next 3 min phase, the auditory cue was delivered (CS score). Freezings were automatically recorded. A freezing score was expressed as the percentage of freezing, when the threshold was defined equally through all experiments in each of the five trial blocks.

Statistics

Differences between groups were examined using unpaired two-tailed *t*-tests, and one-way or two-way repeated measurements ANOVA procedures with Fisher's method. Significance levels for each experiment are indicated in the figure legends. Significance in Cell-Titer Blue viability assay, MEA assay, ThT assays and immunofluorescence intensity assay was established using two-tailed *t*-tests.

Additional Materials and methods are in Supplementary data.

Supplementary data

Supplementary data are available at *The EMBO Journal* Online (http://www.embojournal.org).

Acknowledgements

We thank Adrian Lo, Leen Van Aerschot for technical assistance in animal behaviour studies, Elke Maes, Mieke Vanbrabant, Karen Van Keer and Olga Krylychkina for technical assistance in culturing neurons and Sebastian Munck for confocal microscopy and help with data analysis. This work was supported by the Fund for Scientific Research, Flanders; the Artificial SynApse (IWT ASAP), Federal Office for Scientific Affairs, Belgium IUAP P6/43, a Methusalem grant of the KULeuven and the Flemish Government, an MEMOSAD (F2-2007-200611) of the European Union, an FWO Odysseus grant and the Alzheimer Research Trust (ART) UK.

Conflict of interest

The authors declare that they have no conflict of interest.

References

Aizenstein HJ, Nebes RD, Saxton JA, Price JC, Mathis CA, Tsopelas ND, Ziolko SK, James JA, Snitz BE, Houck PR, Bi W, Cohen AD, Lopresti BJ, DeKosky ST, Halligan EM, Klunk WE (2008) Frequent amyloid deposition without significant cognitive impairment among the elderly. *Arch Neurol* **65:** 1509–1517

Aksenov MY, Aksenova MV, Butterfield DA, Hensley K, Vigo-Pelfrey C, Carney JM (1996) Glutamine synthetase-induced enhancement of beta-amyloid peptide A beta (1–40) neurotoxicity accompanied by abrogation of fibril formation and A beta fragmentation. *J Neurochem* **66:** 2050–2056

Annaert W, De Strooper B (2002) A cell biological perspective on Alzheimer's disease. *Annu Rev Cell Dev Biol* **18:** 25–51

Bentahir M, Nyabi O, Verhamme J, Tolia A, Horre K, Wiltfang J, Esselmann H, De Strooper B (2006) Presenilin clinical mutations can affect gamma-secretase activity by different mechanisms. *J Neurochem* **96:** 732–742

Calabrese B, Shaked GM, Tabarean IV, Braga J, Koo EH, Halpain S (2007) Rapid, concurrent alterations in pre- and postsynaptic structure induced by naturally-secreted amyloid-beta protein. *Mol Cell Neurosci* **35:** 183–193

Chamberlain AK, MacPhee CE, Zurdo J, Morozova-Roche LA, Hill HA, Dobson CM, Davis JJ (2000) Ultrastructural organization of amyloid fibrils by atomic force microscopy. *Biophys J* **79:** 3282–3293

Chirgadze YN, Nevskaya NA (1976) Infrared spectra and resonance interaction of amide-I vibration of the paraellel-chain pleated sheets. *Biopolymers* **15:** 627–636

Citron M, Westaway D, Xia W, Carlson G, Diehl T, Levesque G, Johnson-Wood K, Lee M, Seubert P, Davis A, Kholodenko D, Motter R, Sherrington R, Perry B, Yao H, Strome R, Lieberburg I, Rommens J, Kim S, Schenk D *et al* (1997) Mutant presenilins of Alzheimer's disease increase production of 42-residue amyloid beta-protein in both transfected cells and transgenic mice. *Nat Med* **3:** 67–72

Cleary JP, Walsh DM, Hofmeister JJ, Shankar GM, Kuskowski MA, Selkoe DJ, Ashe KH (2005) Natural oligomers of the amyloid-beta protein specifically disrupt cognitive function. *Nat Neurosci* **8:** 79–84

De Strooper B (2007) Loss-of-function presenilin mutations in Alzheimer disease. Talking Point on the role of presenilin mutations in Alzheimer disease. *EMBO Rep* **8:** 141–146

De Strooper B (2010) Proteases and proteolysis in Alzheimer disease: a multifactorial view on the disease process. *Physiol Rev* **90:** 465–494

Duff K, Eckman C, Zehr C, Yu X, Prada CM, Perez-tur J, Hutton M, Buee L, Harigaya Y, Yager D, Morgan D, Gordon MN, Holcomb L, Refolo L, Zenk B, Hardy J, Younkin S (1996) Increased amyloid-beta42(43) in brains of mice expressing mutant presenilin 1. *Nature* **383:** 710–713

Frost D, Gorman PM, Yip CM, Chakrabartty A (2003) Co-incorporation of A beta 40 and A beta 42 to form mixed pre-fibrillar aggregates. *Eur J Biochem* **270:** 654–663

Gong Y, Chang L, Viola KL, Lacor PN, Lambert MP, Finch CE, Krafft GA, Klein WL (2003) Alzheimer's disease-affected brain: presence of oligomeric A beta ligands (ADDLs) suggests a molecular basis for reversible memory loss. *Proc Natl Acad Sci USA* **100:** 10417–10422

Goormaghtigh E, Cabiaux V, Ruysschaert JM (1994) Determination of soluble and membrane protein structure by Fourier transform infrared spectroscopy. II. Experimental aspects, side chain structure, and H/D exchange. *Subcell Biochem* **23:** 363–403

Haass C, Selkoe DJ (1993) Cellular processing of beta-amyloid precursor protein and the genesis of amyloid beta-peptide. *Cell* **75:** 1039–1042

Hardy J, Selkoe DJ (2002) The amyloid hypothesis of Alzheimer's disease: progress and problems on the road to therapeutics. *Science* **297:** 353–356

Harper JD, Lansbury Jr PT (1997) Models of amyloid seeding in Alzheimer's disease and scrapie: mechanistic truths and physiological consequences of the time-dependent solubility of amyloid proteins. *Annu Rev Biochem* **66:** 385–407

Hartley DM, Walsh DM, Ye CP, Diehl T, Vasquez S, Vassilev PM, Teplow DB, Selkoe DJ (1999) Protofibrillar intermediates of amyloid beta-protein induce acute electrophysiological changes and progressive neurotoxicity in cortical neurons. *J Neurosci* **19:** 8876–8884

Hepler RW, Grimm KM, Nahas DD, Breese R, Dodson EC, Acton P, Keller PM, Yeager M, Wang H, Shughrue P, Kinney G, Joyce JG (2006) Solution state characterization of amyloid beta-derived diffusible ligands. *Biochemistry* **45:** 15157–15167

Hu X, Crick SL, Bu G, Frieden C, Pappu RV, Lee JM (2009) Amyloid seeds formed by cellular uptake, concentration, and aggregation of the amyloid-beta peptide. *Proc Natl Acad Sci USA* **106:** 20324–20329

Jan A, Gokce O, Luthi-Carter R, Lashuel HA (2008) The ratio of monomeric to aggregated forms of Abeta40 and Abeta42 is an important determinant of amyloid-beta aggregation, fibrillogenesis, and toxicity. *J Biol Chem* **283:** 28176–28189

Jarrett JT, Lansbury Jr PT. (1993) Seeding 'one-dimensional crystallization' of amyloid: a pathogenic mechanism in Alzheimer's disease and scrapie? *Cell* **73:** 1055–1058

Kakuda N, Funamoto S, Yagishita S, Takami M, Osawa S, Dohmae N, Ihara Y (2006) Equimolar production of amyloid beta-protein and amyloid precursor protein intracellular domain

from beta-carboxyl-terminal fragment by gamma-secretase. *J Biol Chem* **281:** 14776–14786

Kayed R, Head E, Thompson JL, McIntire TM, Milton SC, Cotman CW, Glabe CG (2003) Common structure of soluble amyloid oligomers implies common mechanism of pathogenesis. *Science* **300:** 486–489

Kim J, Onstead L, Randle S, Price R, Smithson L, Zwizinski C, Dickson DW, Golde T, McGowan E (2007) Abeta40 inhibits amyloid deposition *in vivo*. *J Neurosci* **27:** 627–633

Klyubin I, Betts V, Welzel AT, Blennow K, Zetterberg H, Wallin A, Lemere CA, Cullen WK, Peng Y, Wisniewski T, Selkoe DJ, Anwyl R, Walsh DM, Rowan MJ (2008) Amyloid beta protein dimer-containing human CSF disrupts synaptic plasticity: prevention by systemic passive immunization. *J Neurosci* **28:** 4231–4237

Lacor PN, Buniel MC, Furlow PW, Clemente AS, Velasco PT, Wood M, Viola KL, Klein WL (2007) Abeta oligomer-induced aberrations in synapse composition, shape, and density provide a molecular basis for loss of connectivity in Alzheimer's disease. *J Neurosci* **27:** 796–807

Lambert MP, Barlow AK, Chromy BA, Edwards C, Freed R, Liosatos M, Morgan TE, Rozovsky I, Trommer B, Viola KL, Wals P, Zhang C, Finch CE, Krafft GA, Klein WL (1998) Diffusible, nonfibrillar ligands derived from Abeta1-42 are potent central nervous system neurotoxins. *Proc Natl Acad Sci USA* **95:** 6448–6453

Lashuel HA, Hartley D, Petre BM, Walz T, Lansbury Jr PT (2002) Neurodegenerative disease: amyloid pores from pathogenic mutations. *Nature* **418:** 291

Lauren J, Gimbel DA, Nygaard HB, Gilbert JW, Strittmatter SM (2009) Cellular prion protein mediates impairment of synaptic plasticity by amyloid-beta oligomers. *Nature* **457:** 1128–1132

Lesne S, Koh MT, Kotilinek L, Kayed R, Glabe CG, Yang A, Gallagher M, Ashe KH (2006) A specific amyloid-beta protein assembly in the brain impairs memory. *Nature* **440:** 352–357

Mann DM, Iwatsubo T, Cairns NJ, Lantos PL, Nochlin D, Sumi SM, Bird TD, Poorkaj P, Hardy J, Hutton M, Prihar G, Crook R, Rossor MN, Haltia M (1996) Amyloid beta protein (Abeta) deposition in chromosome 14-linked Alzheimer's disease: predominance of Abeta42(43). *Ann Neurol* **40:** 149–156

Martins IC, Kuperstein I, Wilkinson H, Maes E, Vanbrabant M, Jonckheere W, Van Gelder P, Hartmann D, D'Hooge R, De Strooper B, Schymkowitz J, Rousseau F (2008) Lipids revert inert Abeta amyloid fibrils to neurotoxic protofibrils that affect learning in mice. *EMBO J* **27:** 224–233

Ono K, Condron MM, Teplow DB (2009) Structure-neurotoxicity relationships of amyloid beta-protein oligomers. *Proc Natl Acad Sci USA* **106:** 14745–14750

Pike CJ, Overman MJ, Cotman CW (1995) Amino-terminal deletions enhance aggregation of beta-amyloid peptides *in vitro*. *J Biol Chem* **270:** 23895–23898

Pine J (1980) Recording action potentials from cultured neurons with extracellular microcircuit electrodes. *J Neurosci Methods* **2:** 19–31

Potter SM, DeMarse TB (2001) A new approach to neural cell culture for long-term studies. *J Neurosci Methods* **110:** 17–24

Price JL, Morris JC (1999) Tangles and plaques in nondemented aging and 'preclinical' Alzheimer's disease. *Ann Neurol* **45:** 358–368

Qi-Takahara Y, Morishima-Kawashima M, Tanimura Y, Dolios G, Hirotani N, Horikoshi Y, Kametani F, Maeda M, Saido TC, Wang R, Ihara Y (2005) Longer forms of amyloid beta protein: implications for the mechanism of intramembrane cleavage by gamma-secretase. *J Neurosci* **25:** 436–445

Reiman EM, Chen K, Liu X, Bandy D, Yu M, Lee W, Ayutyanont N, Keppler J, Reeder SA, Langbaum JB, Alexander GE, Klunk WE, Mathis CA, Price JC, Aizenstein HJ, DeKosky ST, Caselli RJ (2009) Fibrillar amyloid-beta burden in cognitively normal people at 3 levels of genetic risk for Alzheimer's disease. *Proc Natl Acad Sci USA* **106:** 6820–6825

Saido TC, Yamao-Harigaya W, Iwatsubo T, Kawashima S (1996) Amino- and carboxyl-terminal heterogeneity of beta-amyloid peptides deposited in human brain. *Neurosci Lett* **215:** 173–176

Sato T, Dohmae N, Qi Y, Kakuda N, Misonou H, Mitsumori R, Maruyama H, Koo EH, Haass C, Takio K, Morishima-Kawashima M, Ishiura S, Ihara Y (2003) Potential link between amyloid beta-protein 42 and C-terminal fragment gamma 49–99 of beta-amyloid precursor protein. *J Biol Chem* **278:** 24294–24301

Scheuner D, Eckman C, Jensen M, Song X, Citron M, Suzuki N, Bird TD, Hardy J, Hutton M, Kukull W, Larson E, Levy-Lahad E, Viitanen M, Peskind E, Poorkaj P, Schellenberg G, Tanzi R, Wasco W, Lannfelt L, Selkoe D *et al* (1996) Secreted amyloid beta-protein similar to that in the senile plaques of Alzheimer's disease is increased *in vivo* by the presenilin 1 and 2 and APP mutations linked to familial Alzheimer's disease. *Nat Med* **2:** 864–870

Schilling S, Zeitschel U, Hoffmann T, Heiser U, Francke M, Kehlen A, Holzer M, Hutter-Paier B, Prokesch M, Windisch M, Jagla W, Schlenzig D, Lindner C, Rudolph T, Reuter G, Cynis H, Montag D, Demuth HU, Rossner S (2008) Glutaminyl cyclase inhibition attenuates pyroglutamate Abeta and Alzheimer's disease-like pathology. *Nat Med* **14:** 1106–1111

Shankar GM, Li S, Mehta TH, Garcia-Munoz A, Shepardson NE, Smith I, Brett FM, Farrell MA, Rowan MJ, Lemere CA, Regan CM, Walsh DM, Sabatini BL, Selkoe DJ (2008) Amyloid-beta protein dimers isolated directly from Alzheimer's brains impair synaptic plasticity and memory. *Nat Med* **14:** 837–842

Snyder SW, Ladror US, Wade WS, Wang GT, Barrett LW, Matayoshi ED, Huffaker HJ, Krafft GA, Holzman TF (1994) Amyloid-beta aggregation: selective inhibition of aggregation in mixtures of amyloid with different chain lengths. *Biophys J* **67:** 1216–1228

Stett A, Egert U, Guenther E, Hofmann F, Meyer T, Nisch W, Haemmerle H (2003) Biological application of microelectrode arrays in drug discovery and basic research. *Anal Bioanal Chem* **377:** 486–495

Suzuki N, Cheung TT, Cai XD, Odaka A, Otvos Jr L, Eckman C, Golde TE, Younkin SG (1994) An increased percentage of long amyloid beta protein secreted by familial amyloid beta protein precursor (beta APP717) mutants. *Science* **264:** 1336–1340

Terry RD, Masliah E, Salmon DP, Butters N, DeTeresa R, Hill R, Hansen LA, Katzman R (1991) Physical basis of cognitive alterations in Alzheimer's disease: synapse loss is the major correlate of cognitive impairment. *Ann Neurol* **30:** 572–580

Tew DJ, Bottomley SP, Smith DP, Ciccotosto GD, Babon J, Hinds MG, Masters CL, Cappai R, Barnham KJ (2008) Stabilization of neurotoxic soluble beta-sheet-rich conformations of the Alzheimer's disease amyloid-beta peptide. *Biophys J* **94:** 2752–2766

Walsh DM, Klyubin I, Fadeeva JV, Cullen WK, Anwyl R, Wolfe MS, Rowan MJ, Selkoe DJ (2002) Naturally secreted oligomers of amyloid beta protein potently inhibit hippocampal long-term potentiation *in vivo*. *Nature* **416:** 535–539

Wang R, Wang B, He W, Zheng H (2006) Wild-type presenilin 1 protects against Alzheimer's disease mutation-induced amyloid pathology. *J Biol Chem* **29:** 29

Wogulis M, Wright S, Cunningham D, Chilcote T, Powell K, Rydel RE (2005) Nucleation-dependent polymerization is an essential component of amyloid-mediated neuronal cell death. *J Neurosci* **25:** 1071–1080

Yan Y, Wang C (2007) Abeta40 protects non-toxic Abeta42 monomer from aggregation. *J Mol Biol* **369:** 909–916

Yoshiike Y, Chui DH, Akagi T, Tanaka N, Takashima A (2003) Specific compositions of amyloid-beta peptides as the determinant of toxic beta-aggregation. *J Biol Chem* **278:** 23648–23655

